International Journal of Mass Spectrometry 275 (2008) 55–63

Contents lists available at ScienceDirect

International Journal of Mass Spectrometry

journal homepage: www.elsevier.com/locate/ijms

VUV photoionisation of free azabenzenes: Pyridine, pyrazine, pyrimidine, pyridazine and s-triazine

G. Vall-llosera[a,*], M. Coreno[b], P. Erman[a], M.A. Huels[c], K. Jakubowska[a], A. Kivimäki[d], E. Rachlew[a], M. Stankiewicz[e]

[a] Royal Institute of Technology, Department of Physics, School of Engineering Sciences, 10691 Stockholm, Sweden
[b] CNR-IMIP, Montelibretti, 00016 Rome, Italy
[c] Ion Reaction Laboratory, Department of Nuclear Medicine and Radiobiology, Faculty of Medicine and Health Sciences, University of Sherbrooke, Sherbrooke, Quebec, Canada J1H5N4
[d] CNR-INFM, TASC Laboratory, 34012 Trieste, Italy
[e] Instytut Fizyki im. Mariana Smoluchowskiego, Uniwersytet Jagielloński, ul. Reymonta 4, 30-059 Kraków, Poland

ARTICLE INFO

Article history:
Received 4 February 2008
Received in revised form 12 May 2008
Accepted 13 May 2008
Available online 23 May 2008

Keywords:
Gas phase
Aromatic rings
Photolysis
Synchrotron radiation

ABSTRACT

Photoionisation mass spectrometry was used to obtain the fragmentation pathways of pyridine, pyridazine, pyrimidine, pyrazine and s-triazine molecules upon absorption of 23.0, 15.7 and 13.8 eV synchrotron photons. The ionic fragments observed vary from molecule to molecule, however $C_2H_2^+$, HCN^+ and $HCNH^+$ are common to all five molecules at the three photon energies. Furthermore, the presence of $C_2H_2N_2^+$, $C_3H_3N^+$ and $C_4H_4^+$ in the spectra of some of the molecules suggests dissociation pathways via loss of HCN moieties. The respective parent cations, $m/q = 79$, 80 and 81 have a greater yield at low photon energies when compared to the most intense fragment peak in each spectra. We recorded two of the fragment cation yields, as well as the parent photoion yield curves of pyridine, pyridazine, and pyrimidine in the 8–30 eV range. The formation of abundant cation fragments show a strong propensity of the molecules for dissociation after the absorption of VUV photons higher than 14 eV. The differences in relative fragment yields from molecule to molecule, and when changing the excitation energy, suggest significant bond rearrangements and nuclear motion during the dissociation time. Thus, bond cleavage is dependent on the photon energy deposited in the molecule and on intramolecular reactivity. With the aid of photoion yield curves and energy estimations we have assigned major peaks in the spectra and discussed their fragmentation pathways.

1. Introduction

The azabenzene family comprises low-Z aromatic molecules structurally related to benzene wherein one or more CH groups in the six-membered ring is replaced by a nitrogen atom (see Fig. 1). In this manner, pyridine is the simplest azabenzene with one N atom substituted, followed by pyridazine, pyrimidine and pyrazine with 2 N atoms substituted in the 1,2-, 1,3- and 1,4- positions, respectively, and s-triazine which has 3 N atoms substituted in the 1,3,5-positions. Pyridine, s-triazine and pyridazine are starting materials in the synthesis of compounds used as intermediates in the production of insecticides and herbicides. Pyridazine, pyridine and pyrazine are also found within the structure of several pharmaceutical drugs. Pyrimidine is the precursor of cytosine, thymine, and uracil in DNA and RNA. Nitrogen heterocycles, such as the ones studied here, have been identified in meteoritic organic matter [1] and it is likely that they are formed when HCN addition occurs during the astronomical production of benzene [2]. Hence, their spectroscopic properties are the base to understand the effects of ionising radiation damage of larger systems in which they are embedded, and to decipher the origin of the interstellar medium.

In the literature we find early evidences of the azabenzenes in a mass fragmentation study of pyridine recorded after 72 eV electron impact [3]. In that study, the probabilities of formation of the various ions produced from pyridine were compared to the mass spectrum of benzene in order to gain understanding of the molecular structure of the benzene molecule. Later on, Fridh et al. [4] initiated a study of s-triazine and other azabenzenes aiming to understand the chemical bonding in benzene. In their study, photoelectron spectra with He I and He II lines, electron energy loss spectra, and mass spectra as a function of the energy absorbed during charge exchange with positive ions of low kinetic energy were recorded for the five azabenzenes investigated here with synchrotron photons. Among the fragments recorded in their study,

* Corresponding author.
E-mail address: gvall.llosera@gmail.com (G. Vall-llosera).

1387-3806/$ – see front matter © 2008 Elsevier B.V. All rights reserved.
doi:10.1016/j.ijms.2008.05.019

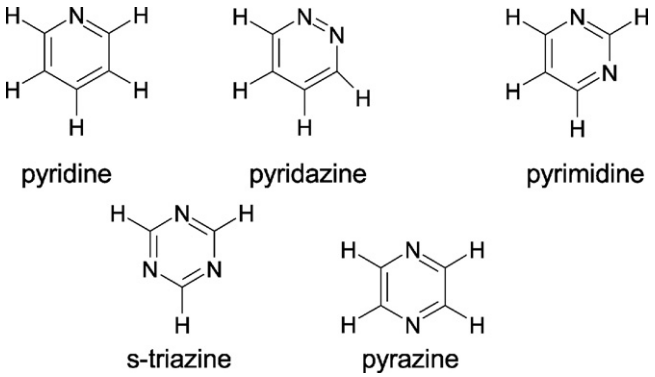

Fig. 1. Sketch of the molecules studied in this work; pyridine ($m/q = 79$), pyridazine ($m/q = 80$), pyrimidine ($m/q = 80$), s-triazine ($m/q = 81$) and pyrazine ($m/q = 80$).

$m/q = 54^+$, 53^+ and 52^+ were concluded to be formed during the loss of an HCN moiety by the corresponding parent cation. It is by now well established in the literature that the loss of HCN due to laser photolysis at fixed wavelengths is one of the major dissociative channels for pyridine [5], pyrimidine [6], pyrazine [7] and s-triazine [8–10]. In all these systems three body dissociation channels produce HCN molecules, a process that becomes dominant in s-triazine (3 N atoms) [9] whilst for pyridine (1 N atom) and pyrimidine (2 N atoms) two body dissociation processes are more common [6]. Two complete VUV photochemistry studies of the DNA bases with synchrotron radiation (SR) were done by Schwell et al. [11] and Jochims et al. [12]. In their mass spectrometry studies of the purinic base adenine, and the pyrimidinic bases, thymine and uracil, they found that the main neutral loss species for adenine is HCN. They also observed that the s-triazine molecule is produced as an intermediate product after irradiation of adenine with 20 eV photons. Several pathways leading to the formation of HCN were also discussed for the pyrimidinic bases, thymine and uracil. Yet another cation fragment, $HCNH^+$ was seen to be produced as an end product via several fragmentation pathways in all three nucleobases. For the adenine molecule, this fragment, $HCNH^+$ was the most intense in their mass fragmentation spectrum. The photofragmentation spectra of the pyrimidinic DNA base cytosine was measured with noble gas resonance radiation at energies from 8.43 to 21.2 eV by Plekan et al. [13]. In their study irradiation with lower photon energies led to softer ionisation and reduced fragmentation. In particular, photoionisation below 16.67 eV led predominantly to the parent ion formation.

In this work we have performed a detailed investigation of the dissociation pathways of five azabenzenes during 8–30 eV monochromatic photon impact using synchrotron radiation, and we find that a large number of different fragments are produced after absorption of VUV photons. Several of the fragmentation products are seen to be formed after simple bond cleavage of the parent molecule, e.g. $HCNH^+$, $C_2HN_2^+$, $C_3H_2N^+$, $C_4H_3^+$, or proceed via neutral HCN loss, e.g., $C_2H_2N_2^+$, $C_3H_3N^+$, $C_4H_4^+$. However, some of the fragments, for example C_3HN^+, C_2HN^+ involve significant bond rearrangement and nuclear motion (atom scrambling) during the dissociation time as also seen for the six membered ring molecule, 2-deoxy-D-ribose (dR) in the pyranose form upon VUV photoabsorption [14]. Contrary to what was seen for dR, where the $(p–H)^+$ and p^+ were not observed, here for the azabenzenes the $(p–H)^+$ and p^+ are clearly formed, plus their signal is enhanced at lower excitation energies when compared to the most intense fragment peak in the spectra. This suggests that six membered rings with N heteroatoms (like DNA ring bases) are more stable upon soft valence ionisation [12,13] compared to six membered rings with O heteroatoms, like DNA sugars. In the photoion yield curves, one or more broad structures occur in the 14–22 eV region in the parent monocation yield and a single feature for fragment ions. Based on these observations we have derived possible fragmentation pathways, calculated their energy balance, and compared them for the different electronic systems.

2. Experimental details

The experiments were performed at beamline 52 of the MAX I synchrotron ring in Lund, Sweden. The combination of a bending magnet and a 1 m normal incidence monochromator enable us to work in the photon energy range of 5–30 eV [15]. The entrance and exit slits of the monochromator were set to 400/400 μm for the whole experiment giving a resolution of 0.13 eV at $h\nu = 22.5$ eV.

The experimental set up for mass spectrometry is described elsewhere in more detail [14,16]. Briefly, it consists of a high-vacuum triple-cross chamber where the crosses are arranged such that the first one is attached to the end of the beamline and connects to the second chamber via a glass capillary in order to guide the beam to the interaction region and also to act as a differential pumping stage. The interaction region is located in the centre of the third chamber, a six-way cross. A quadrupole mass spectrometer (VG-300SPX) is placed on the top flange and a repeller plate at the bottom port provides a constant positive voltage equivalent to 20 V/cm electric field. This last element faces the quadrupole mass spectrometer (QMS) in order to gently drive the ions from the interaction region towards the QMS entrance. The QMS is used in two different modes: scanning mode, where the yield of ionic fragments is recorded as a function of the ion mass/charge ratio at fixed photon energy, and a fixed mass mode, where the QMS is held at a constant mass and we record the ion intensity whilst varying the photon energy (yield of the fragment). In this cross-beam geometry the target gas nozzle is perpendicular to the plane formed by the synchrotron radiation and the central axis of the QMS. The flow of gas is controlled by an external leak valve.

The samples were purchased from Sigma-Aldrich with a stated purity of $> 99\%$ for pyridine and pyrazine, 99% for pyrimidine, 98% for pyridazine and 97% for s-triazine. Pyridine, pyrimidine and pyridazine are liquid at room temperature whilst pyrazine and s-triazine are solid. All samples were subjected to several freeze–pump–thaw cycles in situ to eliminate all traces of contaminants. Despite that, we detected some residual air contamination, i.e., small presence of $O_2^+(m/q = 32)$ in the pyridine, pyridazine, pyrazine and s-triazine spectra at the three measured energies. We have corrected the intensity of $m/q = 28$ fragments for possible contributions from background gas N_2^+ using the O_2^+ peak as a benchmark and the ratio $O_2/N_2 = 1/4$, for $h\nu = 23$ and 15.7 eV, since the N_2^+ threshold of formation is 15.6 eV [17]. In this manner, all of the $m/q = 28$ signal at 13.8 eV is due to $HCNH^+$. The results for the total and partial ion yields are corrected to the variations of the incident photon flux measured with an unbiased Au mesh located prior to our experimental chamber. The absolute transmission through the QMS is not known and we are aware of the lower detection efficiency of ions with high kinetic energies, thus, unless stated otherwise, any comparison between peaks in the same spectrum is always relative to the most intense peak in each spectrum. When comparing the intensity of fragments formed from s-triazine in this study to the fragments formed from adenine in ref. [12] we have first normalised to the most intense peak in each spectra and then compared the percentages.

3. Results and discussion

Three types of relaxation processes following the absorption of VUV photons are of interest to us: (1) ionisation to form the par-

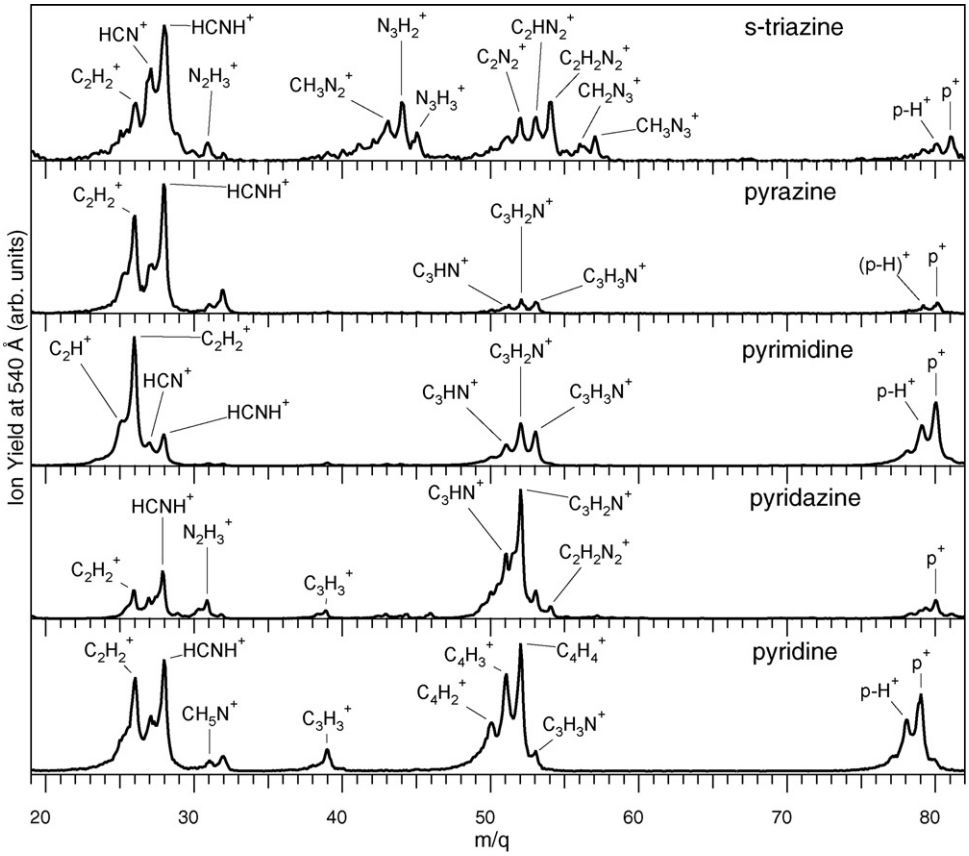

Fig. 2. Fragmentation patterns of s-triazine, pyrazine, pyrimidine, pyridazine and pyridine at 540 Å (23.0 eV). p^+ stands for the parent cation. Major fragments are labelled for each molecule.

ent ion ($M + h\nu \rightarrow M^+ + e^-$), (2) autoionisation ($M + h\nu \rightarrow M^* \rightarrow M^+ + e^-$), and (3) dissociative ionisation ($M + h\nu \rightarrow (M^+)^* + e^- \rightarrow A^+ + e^- + B$). The first and second processes will yield the formation of parent cations and the third one the numerous ionic fragments recorded in our spectra. Dissociative ionisation of a molecule usually takes place in aromatic heterocyclics by ionisation of the heteroatom, followed by charge transfer [18]. In this case, the ring opens and linear fragments will be formed as shown here. It is also known that, in theory, any of these molecules can have two possible cations at some masses, for example $m/q = 27$, $C_2H_3^+$/HCN^+. In a study of pyridine and deuterated pyridine upon electron impact made by Jiao et al. [19] they found that for most of the fragment masses only one cation was present, the other being absent or negligibly small. In the following, the ionic fragments are discussed starting with the low mass and relating them to the presence of complementary fragments. When both complementary fragments are seen as cations the charge '+' is written in brackets, meaning that the charge can localise on either of the fragments. Throughout the discussion we have supposed that the parent molecule is ionised in a first step (ionisation potentials given in Fig. 3) leaving the parent cation either in the ground state or in an excited state. In the case where the parent cation is left in a dissociative excited state, it may fragment, and the charge will localise on either of the fragments. In this work, we have also analysed the energy balances for the formation of each fragment, and they will be discussed in turn.

3.1. Mass spectra

Fig. 2 shows the fragmentation patterns of the five azabenzenes after excitation with 540 Å (23.0 eV) photons. The most intense fragments are labelled for each molecule. Tables 1–5 show the relative intensities of each m/q peak observed in this study at different energies for the five molecules studied here.

3.1.1. Fragments with $25 \leq m/q \leq 32$

The fragment with $m/q = 25$ is seen to be produced from pyrazine, pyrimidine and pyridine (see Fig. 2 and Tables 2, 3 and 5). It is assigned to $C_2H^+$and the fragmentation pathways leading to its formation are different for the different nitrogen containing molecules. For pyridine the fragmentation pathway can be $C_2H^+ (m/q = 25) + C_3H_4N (m/q = 54)$, in agreement with the electron impact study made by Jiao et al. [19]. For the diazines two possible fragmentation pathways can lead to the formation of C_2H^+,

$$(a)\ p^+ \rightarrow C_2H^+ (m/q = 25) + C_2H_3N_2 (m/q = 55)$$

where the complementary fragment emerges as a neutral, or

$$(b)\ p^+ \rightarrow (p - 1)^+ (m/q = 79) + H$$
$$\rightarrow HCN (m/q = 27) + C_3H_2N^+ (m/q = 52) + H$$

and then

$$C_3H_2N^+ (m/q = 52) \rightarrow HCN (m/q = 27) + C_2H^+ (m/q = 25)$$

where the successive loss of HCN by the (p–H) cation leads to $C_2H^+ (m/q = 25)$. Further evidence for this dissciation channel in pyrimidine and pyrazine is the presence of the intermediate fragment, $m/q = 52$ ($C_3H_2N^+$) in our spectra. Direct formation of C_2H^+ occurs when the parent dissociates, e.g. $p^+ \rightarrow C_2H^+$+fragment. The respective complementary fragments for pyridine and the two

Table 1
Fragments observed for the s-triazine molecule after absorption of VUV photons

m/q	Tentative assignment	Relative intensity		
		23.0 eV	15.7 eV	13.8 eV
16	O^+	0	0	0
26	$C_2H_2^+$	10	10	1
27	HCN^+	40	30	20
28	$HCNH^+$	100	100	30
31	$N_3H_3^+$	25	25	20
32	O_2^+	10	10	0
41	CHN_2^+	10	0	0
42	$CH_2N_2^+$	7	0	0
43	$CH_3N_2^+$	25	25	10
44	$N_3H_2^+$	50	45	40
45	$N_3H_3^+$	30	20	15
51	C_3HN^+	10	0	0
52	$C_2N_2^+$	30	35	10
53	$C_2HN_2^+$	30	40	30
54	$C_2N_2^+$	60	80	70
55	CHN_3^+	10	0	0
56	$CH_2N_3^+$	15	0	0
57	$CH_3N_3^+$	25	25	25
79	$C_3HN_3^+$	5	20	25
80	$C_3H_2N_3^+$	15	40	50
81	$C_3H_3N_3^+$	25	70	100

Intensities are relative to the strongest fragment in each spectrum which has an intensity of 100. The relative peak intensities are derived from the individual peak curves (resolved by fitting modified Gaussian functions to each peak at each of the photon energies) with an accuracy of ca 30%. In s-triazine $m/q = 32$ cannot be created from the molecule, thus $m/q = 32$ is O_2^+, and the intensity of the $m/q = 28$ peak at 23 and 15.7 eV has been corrected by subtracting the contribution of N_2^+ in air relative to the O_2^+ measured here as explained in the experimental section.

Table 2
Fragments observed for the pyrazine molecule after absorption of VUV photons

m/q	Tentative assignment	Relative intensity		
		23.0 eV	15.7 eV	13.8 eV
16	O^+	10	0	0
25	C_2H^+	15	20	25
26	$C_2H_2^+$	100	100	10
27	HCN^+	20	35	40
28	$HCNH^+$	25	0	75
31	$N_2H_3^+$	10	15	40
32	O_2^+	30	30	45
51	C_3HN^+	10	5	10
52	$C_3H_2N^+$	15	30	40
53	$C_3H_3N^+$	13	50	75
78	$C_4H_2N_2^+$	0	5	0
79	$C_4H_3N_2^+$	10	15	50
80	$C_4H_4N_2^+$	12	35	100

Intensities are relative to the strongest fragment in each spectrum which has an intensity of 100. Intensities are derived as described in Table 1 and in Section 2.

Table 3
Fragments observed for the pyrimidine molecule after absorption of VUV photons

m/q	Tentative assignment	Relative intensity		
		23.0 eV	15.7 eV	13.8 eV
25	C_2H^+	5	5	0
26	$C_2H_2^+$	100	50	10
27	HCN^+	20	15	5
28	$HCNH^+$	25	10	<1
31	$N_2H_3^+$	0.3	0	2
51	C_3HN^+	10	6	2
52	$C_3H_2N^+$	30	30	25
53	$C_3H_3N^+$	25	50	35
78	$C_4H_2N_2^+$	5	8	5
79	$C_4H_3N_2^+$	25	40	30
80	$C_4H_4N_2^+$	45	100	100

Intensities are relative to the strongest fragment in each spectrum which has an intensity of 100. Intensities are derived as described in Table 1 and in Section 2.

Table 4
Fragments observed for the pyridazine molecule after absorption of VUV photons

m/q	Tentative assignment	Relative intensity		
		23.0 eV	15.7 eV	13.8 eV
16	O^+	0	0	0
26	$C_2H_2^+$	20	86	5
27	HCN^+	10	10	5
28	$HCNH^+/N_2^+$	20	10	20
31	$N_2H_3^+$	15	20	70
32	O_2^+	<5	<5	5
39	$C_3H_3^+$	5	5	5
43	$CH_3N_2^+$	3	3	0
51	C_3HN^+	15	15	45
52	$C_3H_2N^+/C_4N_4^+$	100	100	100
53	$C_3H_3N^+$	15	20	40
54	$C_2H_2N_2^+$	10	10	45
79	$C_4H_3N_2^+$	3	10	3
80	$C_4H_4N_2^+$	15	20	75

Intensities are relative to the strongest fragment in each spectrum which has an intensity of 100. Intensities are derived as described in Table 1 and in Section 2.

Table 5
Fragments observed for the pyridine molecule after absorption of VUV photons

m/q	Tentative assignment	Relative intensity		
		23.0 eV	15.7 eV	13.8 eV
16	O^+	<1	0	<1
25	C_2H^+	15	0	0
26	$C_2H_2^+$	70	5	10
27	HCN^+	30	10	10
28	$HCNH^+$	45	<5	40
31	CH_5N^+	7	10	10
32	O_2^+	10	15	15
39	$C_3H_3^+$	17	10	0
50	$C_4H_2^+$	38	5	3
51	$C_4H_3^+$	47	15	20
52	$C_4H_4^+$	100	100	75
53	$C_3H_3N^+$	15	15	3
78	$C_5H_4N^+$	24	30	15
79	$C_5H_5N^+$	63	75	100

Intensities are relative to the strongest fragment in each spectrum which has an intensity of 100. Intensities are derived as described in Table 1 and in Section 2.

diazines are $m/q = 54$ (C_3H_4N) and $m/q = 55$ ($C_2H_3N_2$), respectively, which are not seen as cations. Thus if this channel occurs, it leaves behind a neutral fragment.

The ion fragment with $m/q = 26$ is seen to be produced from all molecules at all excitation energies (see Fig. 2 and Tables 1–5). This mass has two possible cations, $CN^+$and $C_2H_2^+$. Drawings of these two dissociation pathways and thermodynamic energy balances are shown in Fig. 3 reaction I. In order to obtain the values shown in Fig. 3 we have used bond dissociation energies (BDE) as related in Table 6. In the formation of $CN^+$from pyridine for instance, three bonds need to be broken; one C— N, one C— C and one C— H. According to the BDE values in Table 6, to break a C— N bond

Table 6
Compilation of bond strengths used in this work

Bond type	BDE (kcal/mol)	BDE (eV)	Reference
C— C	83	3.6	[24]
N— N	38.4	1.7	[24]
C— H	105	4.5	[25]
C— N	73	3.2	[24]
N═ N	109	4.7	[24]
C═ N	147	6.4	[24]
C═ C	146	6.3	[24]
N— H	93	4.0	[24]
C≡ C	200	8.7	[24]
N≡ N	226	9.8	[24]

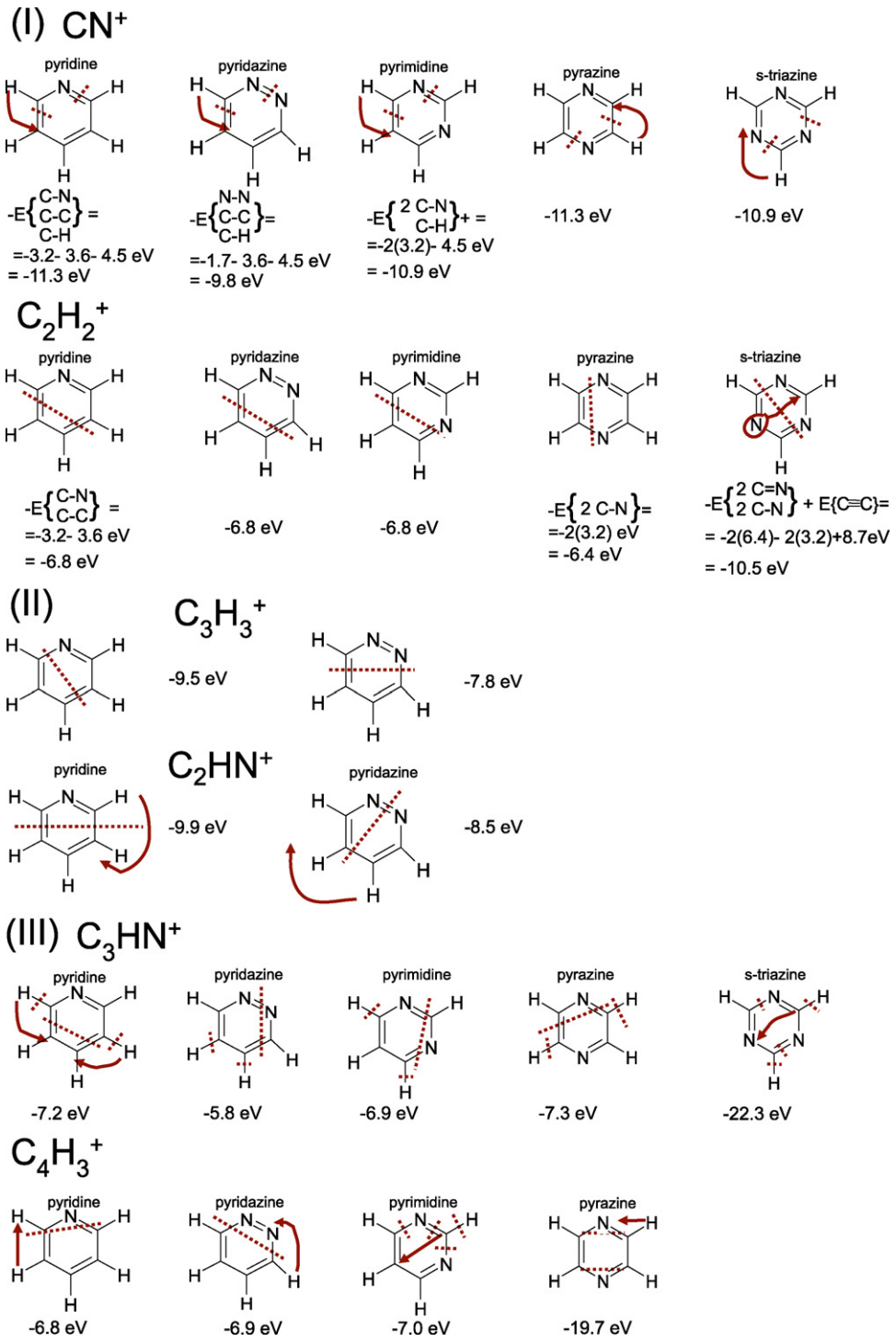

Fig. 3. Some of the fragmentation channels observed here: (I) is discussed in $m/q = 26$; (II) corresponds to $m/q = 39$ and 42; (III) are the thermodynamics of $m/q = 51$. Table 6 compiles the bond dissociation energies we have used in this work for the detailed calculation of the thermodynamic energy balances. Negative values mean an endothermic process, and do not include the ionisation potential of the respective parent molecule. Thus, for a total thermodynamic estimation the respective ionisation potentials (in negative value) of 10.01 eV [4] for s-triazine, 9.29 eV [21] for pyrazine, 9.3 [22,21] for pyrimidine, 8.7 eV [23,21] and 9.3 eV [20,21] for pyridine have to be added to the energy balance.

an average energy value of 3.2 eV is needed. The addition of 3.6 and 4.5 eV for the breakage of the C—C and C— H bond respectively, gives a total value of −11.3 eV. This value does not include the ionisation energy of the parent molecule, 9.3 eV [20,21]. Thus, the nominal thermodynamic threshold calculated here for the formation of CN^+ from pyridine is $-(11.3 + 9.3) = -20.6$ eV. The negative values obtained here and in Fig. 3 indicate the endothermicity of the process (here we neglect for the moment the exothermicity of intra-molecular concerted bond rearrangements which occur during the dissociation process, and which lower the formation thresholds; these will be discussed at a later point in the paper for the $m/q = 28$ fragment). Looking at Fig. 3 reaction I, we observe that the thermodynamic energy values for all five molecules are lower for the $C_2H_2^+$ formation channel as opposed to CN^+ for-

mation, therefore peak $m/q = 26$ is assigned to $C_2H_2^+$. This is in agreement with the study made by Jiao et al. [19] for pyridine where they also assign $m/q = 26$ to $C_2H_2^+$. Pyridine's complementary neutral fragment of the $m/q = 26$ cation fragment is $m/q = 53$ which is clearly seen as a cation in our spectra, also in agreement with ref. [20] and assigned here to $C_3H_3N^+$ (see further in the text). The intensity ratio between these two fragments, $C_2H_2^+(m/q = 26)$ and $C_3H_3N^+$ $(m/q = 53)$, in pyridine at different energies is seen to be as follows: $I(53)/I(26) > 1$ at 790 Å (15.7 eV) and < 1 at 540 and 900 Å (23.0 and 13.8 eV respectively) (see Table 5). This suggests that at 790 Å $m/q = 26$ formation is the predominant channel, whilst at 540 and 900 Å $m/q = 53$ is produced more efficiently. In the diazines, the fragmentation pathway proposed here is $C_2H_2^+(m/q = 26) + C_2H_2N_2$ $(m/q = 54)$. This complementary fragment $(m/q = 54)$ is only weakly seen as a cation in the pyridazine spectra (see Fig. 4) and assigned to $C_2H_2N_2^+$. The dissociation pathway in s-triazine is $C_2H_2^+$ $(m/q = 26) + CHN_3$ $(m/q = 55)$; here the latter neutral fragment is very weakly seen as a cation, i.e., the dissociation pathway of s-triazine as shown in Fig. 3 reaction I is in favour of $C_2H_2^+$ production.

The fragment with $m/q = 27$ is seen to be produced from all five molecules at all three energies (see Fig. 2 and Tables 1–5). This mass has also two cations, namely $C_2H_3^+$ and HCN^+. It is seen in ref. [11] that in pyrimidine, HCN elimination dominates despite the fact that it requires rupture of at least two bonds. One of the reasons is the thermodynamic stability of HCN. According to our calculated thermodynamic energy values, and also in agreement with refs. [12,19,22], the $m/q = 27$ fragment is attributed here predominantly to HCN^+ in all five molecules. In the s-triazine molecule HCN^+ $(m/q = 27)$ is directly produced when the parent cation looses 2 neutral HCN groups, i.e., $C_3H_3N_3^+$ $(m/q = 81) \rightarrow HCN + C_2H_2N_2^+$ $(m/q = 54)$, $C_2H_2N_2^+$ $(m/q = 54) \rightarrow HCN + HCN^+$ $(m/q = 27)$. Note that the complementary intermediate fragment for s-triazine $m/q = 54$, assigned here to $C_2H_2N_2^+$, is formed during the first loss of HCN by the parent cation, and is strongly seen in the mass spectra (see Fig. 2 and Table 1). For pyridine, the complementary fragment of $m/q = 27$ is $m/q = 52$, which is assigned here to $C_4H_4^+$, in agreement with refs. [5,19]. This complementary fragment, $C_4H_4^+$ $(m/q = 52)$ is strongly present as a cation in our spectra (see Fig. 2 and Table 5). For the diazines, the complementary fragment of $m/q = 27$ corresponds to $m/q = 53$, assigned to $C_3H_3N^+$ in agreement with [6], and present in all the diazine mass spectra (see Fig. 2 and Tables 2–4).

Fragments with $m/q = 28$ are observed from all five molecules and are assigned here to $HCNH^+$ (see Fig. 2 and Tables 1–5). When calculating the relative intensity of $m/q = 28$ for all the molecules studied here at 23 and 15.7 eV we have considered a contribution from the background gas at the ratio of: $N_2/O_2 = 1/4$ according to ref. [17], and we have subtracted its contribution from the intensity of $m/q = 28$ (see Tables 1–5 and Section 2). In the pyridine molecule, the formation of $HCNH^+(m/q = 28)$ proceeds via formation of HCN^+ $(m/q = 27)$ which picks up a H atom during the dissociation leaving a neutral $m/q = 51$ fragment behind (see Fig. 3 reaction III for the formation of $m/q = 51$). In the ion charge exchange study of ref. [20] they detected the cation fragment $m/q = 51$ which they assign to $C_4H_3^+$. Considering a 2-body fragmentation process, then the complementary fragment of $m/q = 51$ is $m/q = 28$ and it can unambiguously be assigned to HCNH. In the diazines, three cations could be present in the formation of the peak at $m/q = 28$; (a) $C_2H_4^+$, (b) $HCNH^+$ and (c) N_2^+. Upon inspection of the geometry of the molecules (see Figure 1), if N_2^+ is to be formed, it would only be favourable from the pyridazine molecule, because of the position of the two N atoms in the molecule. Considering the nominal thermodynamic thresholds we observe that, in pyridazine the formation of $C_2H_4^+$ has the highest thermodynamic threshold with −7.2 eV, followed by the formation of N_2^+ which requires 6.4 eV (breakage of 2 C— N bonds) and finally $HCNH^+$ requiring 4.9 eV. Here, for the $C_2H_4^+$ and $HCNH^+$ thermodynamic thresholds, the formation of new bonds has been taken into account. For instance, the formation of $C_2H_4^+$ requires the breakage of two C— C and two C— H bonds (16.2 eV) but 9 eV are regained when the two atoms attach to the leaving $C_2H_2^+$ giving a total threshold of −7.2 eV. From these values we assign the peak at $m/q = 28$ in pyridazine mainly to the $HCNH^+$ fragment. In the ion charge exchange study of pyridazine by Åsbrink et al. [23] they discussed the formation of $(p–N_2)^+$, in terms of loss of a neutral N_2 molecule by the pyridazine's parent cation for energies above 11.2 eV. This would suggest that some of the intensity of the $m/q = 52$ fragment for pyridazine could be in part due to $C_4H_4^+$, and thus, $m/q = 28$ would be in part attributed to N_2^+. For pyrimidine and pyrazine, the N_2^+ thermodynamic threshold of formation is much higher than the other two ionic fragments, $C_2H_4^+$ and $HCNH^+$, which require about the same energy. Thus formation of N_2^+ is probably suppressed for pyrimidine and pyrazine, and only $C_2H_4^+$ and $HCNH^+$ are likely. Here we are not able to unambiguously assign $m/q = 28$ for pyrimidine and pyrazine, however the presence of $(p–HCN)^+$ $(m/q = 53)$ in our mass spectra and those from refs. [22,26], plus the fact that $HCNH^+$ is formed via loss of the neutral fragment C_3NH_2in the pyrimidine molecule [6], strongly implies that the assignment of $m/q = 28$ here is $HCNH^+$. Its formation proceeds via concerted H atom addition during the formation of HCN^+, since it is well known that H atoms migrate along the molecule [6]. The corresponding complementary fragment for the diazines is $m/q = 52$ which is also recorded here as a cation. In s-triazine, our thermodynamic values also favour $HCNH^+$ $(m/q = 28)$formation, leaving as a complementary fragment $C_2HN_2^+$ $(m/q = 53)$. This is in agreement with the study of s-triazine after charge exchange with positive ions in ref. [4] who assign this peak to $HCNH^+$.

The fragment with $m/q = 31$ is produced from all molecules (see Fig. 2 and Tables 1–5). It is assigned to CH_5N^+, probably in a $[H_3C–NH_2]$ structure for pyridine, and to $N_2H_3^+$ for the diazines and s-triazine according to thermodynamic values calculated here. The lowest thermodynamic threshold is calculated here to be −6.8 eV for the CH_5N^+ ionic fragment produced from pyridine; it follows the formation of $N_2H_3^+$ from pyridazine with −7.9 eV and finally, −12.6 eV for the production of $N_2H_3^+$ from pyrazine, pyrimidine and s-triazine. From these values it is immediately clear that formation of $N_2H_3^+$ from pyridazine is energetically more favourable even at lower incident photon energies, thus its relative intensity is higher than in the pyrazine, pyrimidine and s-triazine molecules. None of the respective complementary fragments, $m/q = 48$ for pyridine, $m/q = 49$ for the diazines and $m/q = 50$ for s-triazine, are seen as cations in the spectra recorded here. Note that the formation of CH_5N^+ from pyridine and $N_2H_3^+$ from all the other four molecules strongly suggest complex bond rearrangement and atom scrambling during the dissociation time.

3.1.2. *Fragments with* $39 \leq m/q \leq 45$

The $m/q = 39$ fragment is strongly present in pyridine and weakly present in pyridazine (see Fig. 2 and Tables 4 and 5). Sketches of the thermodynamics for the two possible cation fragments, $C_3H_3^+$ and C_2HN^+ are shown in Fig. 3 reaction II. According to our values, the formation of $C_3H_3^+$ requires 9.5 eV for pyridine and 7.8 eV for pyridazine, compared to the formation of C_2HN^+ which demands 9.9 eV for pyridine and 8.5 eV for pyridazine. In pyridine and also in agreement wih refs. [5,19,20], the formation of $C_3H_3^+$ is energetically more favourable. The same is true for pyridazine. The complementary fragment of $m/q = 39$ is $m/q = 40$ for pyridine and $m/q = 41$ for pyridazine. None of them are seen as cations in our spectra. Fragments with $m/q = 40$

and 41 are only weakly seen produced from s-triazine at 540 Å (see Fig. 2) and one is the complementary fragment of the other. There are two possible dissociation pathways of the parent cation, (1) $C_2H_2N^+$ ($m/q = 40$) + CHN_2^+ ($m/q = 41$) where the charge can localise on either fragment; (2) CN_2^+ ($m/q = 40$) + $C_2H_3N^+$ ($m/q = 41$). Energetically speaking, the first pathway calls for 9.6 eV whilst to follow the second 10.1 eV are needed. This makes reaction (1) the most favourable.

As almost all fragments around mass 40, the cation fragments with $m/q = 45, 44$ and 43 are only seen in the s-triazine spectra (see Fig. 2 and Table 1). The cation fragment with $m/q = 45$ is assigned here to $N_3H_3^+$. Note that in order to form this molecule every single bond in the parent molecule needs to be broken. Thus, looking at the geometry of the molecule (see Fig. 1), the formation of this cation fragment seems highly improbable. Despite that, its formation is assisted energetically when the 3 N atoms and the 3 H atoms bind together to form $N_3H_3^+$. Moreover, the formation of this fragment may become feasible when the N atom out-of-plane vibrational mode of s-triazine is excited [27].

The formation of $m/q = 44$ from s-triazine is assigned here to $N_3H_2^+$. The high mobility of H atoms during the dissociation time [5] and the formation of new bonds as seen for $m/q = 45$ would allow the formation of this fragment. Similarly, $m/q = 43$, weakly produced from s-triazine, could be assigned to N_3H^+ ($m/q = 43$) + C_3H_2 ($m/q = 38$) with an endothermic threshold of 16.8 eV. Alternatively, $m/q = 43$ can also follow the dissociation pathway: $CH_3N_2^+$ ($m/q = 43$) + C_2N ($m/q = 38$) which only requires 10.0 eV (taking into consideration bond formation and rearrangement within the fragments). This suggests $CH_3N_2^+$ as the assigned ionic fragment to $m/q = 43$ for s-triazine. The assignment proposed here is in agreement with ref. [12] which proposes that the formation of $m/q = 43$ follows the pathway, $C_2H_4N_3^+$ ($m/q = 70$) → $CH_3N_2^+$ ($m/q = 43$) + HCN ($m/q = 27$).

3.1.3. Fragments with $m/q = 50$–60

In this mass region, two or three strong peaks can be observed, depending on the molecule. The strongest peak in pyridine is $m/q = 52$ (see Fig. 2 and Table 5) assigned here to $C_4H_4^+$ also in agreement with refs. [19] and [20]. The formation of this fragment follows a neutral HCN loss from the parent cation, $p^+ \rightarrow C_4H_4^+ + HCN^+$. Successive H atom loss from excited $C_4H_4^+$ during the dissociation process will lead to the formation of $C_4H_3^+$ ($m/q = 51$) and $C_4H_2^+$ ($m/q = 50$) and the capture of a H atom from the leaving HCN will lead to the formation of $m/q = 53$, $C_4H_5^+$. Alternatively, the production of $m/q = 51$ from pyridine can also follow the pathway, $(p–H)^+ \rightarrow C_4H_3^+ + HCN^+$, since $(p–H)^+$ is also observed as a cation in the pyridine spectra. The fragment formation pathway and bond rearrangement leading to formation of $m/q = 51$ are shown in Fig. 3 reaction III.

In pyrazine and pyrimidine the two strongest peaks in the $m/q = 50$–60 region are $m/q = 53$ and $m/q = 52$ (see Tables 3 and 2). Here the loss of a neutral HCN (m/q=27) molecule by any of the excited parent cations leads to the formation of $C_3H_3N^+$ ($m/q = 53$) in both molecules. As seen for the pyridine molecule, successive losses of H atoms by $C_3H_3N^+$ ($m/q = 53$) will lead to the formation of $C_3H_2N^+$($m/q = 52$) and of C_3HN^+($m/q = 51$) also seen in the pyrazine and pyrimidine spectra. Pyridazine is an isomer of pyrimidine and pyrazine, thus we would expect $m/q = 53$ to be the strongest in the mass spectra due to one HCN loss in agreement with the results for pyrimidine and pyrazine. Instead the strongest peak in the pyridazine spectra is $m/q = 52$ and attributed here to $C_3H_2N^+$. This fragment is thus formed when the parent cation $m/q = 80$ looses a neutral $m/q = 28$. The two possible pathways for formation of $m/q = 52$ are p^+–HCNH or p^+–N_2, as discussed in Section 3.1.1. The loss of a H atom during the dissociation process leads to the formation of $m/q = 51$ also seen in the pyridazine spectra and attributed here to C_3HN^+. Proceeding in the same manner, the transfer of one or two H atoms from the dissociating neutral complementary fragment will lead to the formation of $C_3H_3N^+$ ($m/q = 53$) or $C_3H_4N^+$ ($m/q = 54$) weakly seen in the pyridazine spectra.

In the s-triazine molecule the strongest peak is $m/q = 54$ and assigned here to $C_2H_2N_2^+$. As in the previous discussion the loss of an HCN molecule by the parent cation leads to the formation of $C_2H_2N_2^+$. Successive losses of H atoms from this cation fragment leads to the formation of $C_2HN_2^+$($m/q = 53$) and $C_2N_2^+$ ($m/q = 52$) also seen in the mass spectra of s-triazine. $m/q = 56$ and 57 are only seen in the s-triazine spectra. The fragment with $m/q = 56$ is assigned to $CH_2N_3^+$ and $m/q = 57$ to $CH_3N_3^+$. With 3 N atoms both fragments are only possible and visible in the s-triazine spectra. The respective fragmentation pathways are $CH_2N_3^+$ ($m/q = 56$) + C_2H ($m/q = 25$) and $CH_3N_3^+$ ($m/q = 57$) + C_2 ($m/q = 24$).

3.1.4. Fragments with $78 \leq m/q \leq 81$

This group of fragments is formed by the parent cations and by the ionic fragments created by loss of one or two neutral H atoms from the parent cation. Indeed, our recorded H- α dispersed fluorescence yield from pyrimidine [16] shows that when a H atom is detached from the parent, this H atom can be created in a neutral excited state ($n = 3$ in this case) and can be detected by its fluorescence. Thus the presence of $C_4H_3N_2^+$ in the pyrimidine spectra here may also be accompanied by detachment of a neutral excited hydrogen atom. Common to all mass spectra in this region, we observe that the relative yield of p^+ and $(p–H)^+$ is greater at low energies (900 Å, 13.8 eV) than at high energies (540 Å, 23.0 eV) due to the fact that the interaction with low energy photons is a more gentle process than with high energy photons, where the ring opening probability upon ionisation is higher.

3.2. Analysis of the ion yield curves

Fig. 4 shows the mass selected photoion yield curves measured here. Three parent cations, pyridine, pyridazine and pyrimidine, and two ionic fragments, $m/q = 52$ for pyridine and $m/q = 26$ for pyrazine are shown. The second order light from the monochromator was not filtered here, thus a minor contribution of this stray radiation can be seen in the yield functions of the fragments $m/q = 52$ and $m/q = 26$ (ca. 11 eV for both), and it may also be present in the parent cation curves.

The profiles of the fragment and parent ion yields (see Fig. 4) can give us further information on the fragmentation pathways of the molecules studied here. As a general trend we observe that the parent cation yield curves have two broad structures between 14 and 21 eV, whilst the ion fragment yields have only one peak at around 22 eV. This is in agreement with the two observed VUV peaks in the 15–20 eV region in the absorption spectrum for the parent cation of the benzene molecule and the single structure observed for the ion fragment yields recorded from benzene and other polycyclic aromatic hydrocarbons (PAHs) after photon absorption in the 8–30 eV region [28].

Additional information from the parent ion yield curves can be extracted comparing them to the photoelectron (PE) spectra of the same molecules in the VUV region. Several photoelectron studies of pyrimidine [22,29,30] reveal spectral features at approximately the same energies as the peak positions in our parent ion yield. In particular, the work done by Potts et al. [30] assigns seven photoelectron bands at 9.8, 10.5, 11.3, 14.0, 15.8, 17.0 and 17.7 eV, respectively, plus some other spectral features at 21 and 24 eV (see the bars in Fig. 5). In analogy to the discussion for adenine [12] relating structures in the PE spectrum to structures in the ion yield

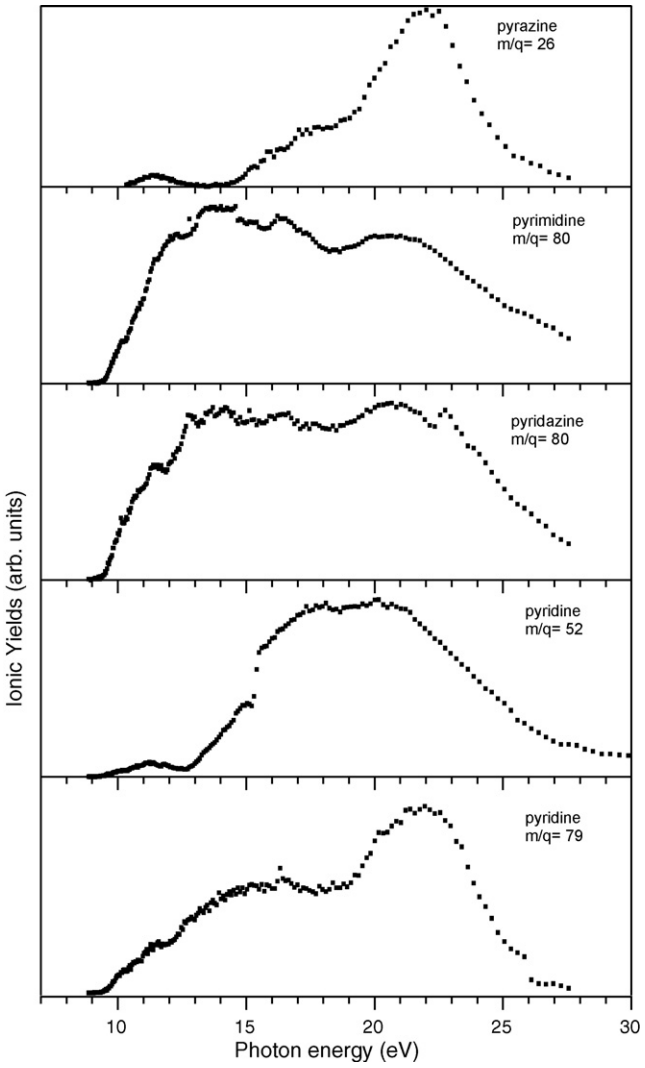

Fig. 4. Mass selected partial ion yields, normalised to the photon flux, for pyrimidine, pyridazine and pyridine parent cations. Two main fragments are also recorded, $m/q = 52$ for pyridine and $m/q = 26$ for pyrazine. The second order light was not filtered here, thus the curves for the two cation fragments show the contribution of this light below 13 eV. The sudden discontinuous increase in signal in the pyridine $m/q = 52$ at 15 eV is due to a recorded pressure burst. The spread in the data points accounts for the counting statistics. However, sample density variations might be causing the small fluctuations seen in the curves.

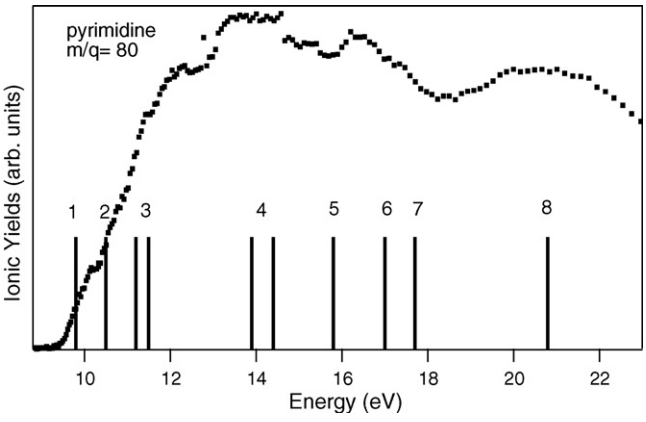

Fig. 5. Parent ion yield of pyrimidine after VUV photon absorption. The vertical bars are assigned photoelectron bands seen at kinetic energies shown in the graph and recorded at 45 eV from ref. [30]. The height of the bands is not relevant, here they are plotted to indicate the kinetic energy positions.

curves, here we propose that the positions of the 4th, 6th and 8th bands in Fig. 5 correspond to the positions of the peaks present in the pyrimidine parent ion yield curve recorded here. This would imply that the electrons detected in the PE spectra are partly from the orbitals of the unfragmented parent molecule (detected here). On the other hand the 7th band in the PE spectra coincides with a minimum in our spectrum which would suggest that the parent ions fragment.

3.3. Comparison to other studies

From the comparison of our study to other works as in the previous sections, as well as with some studies using laser excitation [31,32], we reach the following conclusions:

- the closest resemblance to our study in terms of cracking patterns are the results using electron impact: Jiao's study [19] for pyridine and ref. [33] for pyrazine, pyridazine, pyrimidine and s-triazine; however in disagreement with the studies mentioned above, the cation fragment $m/q = 31$ is seen to be produced, in our study, from all five molecules. In pyridazine we observe additional fragments such as $m/q = 43$ and 54; $m/q = 78$ in pyrimidine, and $m/q = 44$, 45, 51, 56, 57 and 79 in s-triazine, none of which are observed in any of the studies we compared our work to;
- after comparing the relative intensities of the fragments formed here from s-triazine to the the fragments formed from adenine upon 20 eV photon excitation [11,12], we found that in the region below m/q=81, the fragment with $m/q = 28$ is the most intense in both studies and that 10 out of the 12 fragments compared (common to the present and previous studies) have roughly the same relative intensity, e.g., $I(m/q = 53)$ in ref. [12] is 25% of the $m/q = 28$ intensity in adenine, and $I(m/q = 53)$ here is 21% of the $m/q = 28$ fragment intensity. This would suggest that the fragmentation pathway of the DNA base adenine (which is the only base that contains only C, N, and H atoms), upon 20 eV photon impact, undergoes formation of s-triazine which in turn, fragments to smaller cations;
- as already observed by Plekan et al. [13] for cytosine (pyrimidinic DNA base), here we also observe the same trend in all five molecules, namely the lower the photon energy the softer the ionisation, and the higher the yield of parent cation molecules.

4. Conclusions

We have used synchrotron VUV photons and mass spectrometry to investigate the fragmentation pathways of gas phase heteroaromatic rings such as pyridine, pyridazine, pyrimidine, pyrazine and s-triazine. We have found that after absorption of VUV photons the molecules dissociate and yield numerous ionic fragments. In common to all compounds are $C_2H_2^+$, HCN^+ and $HCNH^+$ at all three photon energies. Also, the presence of $C_2H_2N_2^+$ from s-triazine, $C_3H_3N^+$ from the diazines and $C_4H_4^+$ from pyridine in the spectra suggests dissociation pathways via losses of HCN moieties. At low VUV photon energies, we observe a higher relative yield of the five respective parent cations when compared to the most intense peak in each spectra which shows a propensity for the molecule to remain intact. With the aid of thermodynamic energy thresholds, and comparisons to previous experiments recorded in the literature we have assigned most of the main peaks in our mass spectra and discussed their formation pathways. From the analysis of the mass spectra we can conclude that: (1) the behaviour of these azabenzenes upon VUV photon excitation is more related to the behaviour of their most basic structure analogue, benzene, or to DNA bases and other polycyclic hydrocarbons, than to the

behaviour observed for ring biomolecules like the DNA sugar when exposed to VUV ionising radiation [14]. The mass spectra of the azabenzenes studied here show a strong propensity to fragmentation at high VUV energies but are more stable for low VUV photon absorption. This contrasts with the behaviour seen for 2-deoxy-D-ribose, also in the gas phase [14] where strong fragmentation is observed even at low VUV photon energies. In this latter study it is discussed that this strong fragmentation tendency upon VUV photon absorption may lead to single-strand breaks in cellular DNA. From our present study, we propose that six membered rings with N heteroatoms (like pyrimidinic DNA bases) are more stable upon soft valence ionisation, compared to six membered rings with O heteroatoms, like DNA sugars. Thus, our study would suggest that VUV absorption in DNA would lead mainly to sugar damage via single strand break, than base damage. (2) We have determined the survivability of five heterorings in the VUV environment and seen that, VUV photoabsorption by nitrogen-substituted analogues of benzene leads to destruction of these heterorings in the laboratory. Because nitrogen heterocycles possess dipole moment (ca. 2 Debye for pyridine and pyrimidine [2]) they have been observed in the interstellar medium [34,35] and pyrimidines have actually been identified in meteoritic organic matter found here on earth, see [36] and references there in. As we know, pyrimidines play a basic role in terrestrial biochemistry [37] since they are fundamental components of DNA and RNA. Determining their survivability in the presence of ionising radiation in the laboratory may hint at their survivability in space.

Acknowledgements

Financial support from the Swedish Research Council (VR) and the EU program – Access to Research Infrastructure action – (through the MAX laboratory) is gratefully acknowledged. M.A. Huels acknowledges funding from the Natural Science and Engineering Research Council of Canada and the Canadian Space Agency. We acknowledge Stefano Varas and Fabio Suran from the technical electronic services of CNR-INFM, Laboratorio Nazionale TASC, (Trieste, Italy), for their contribution in developing the QMS data acquisition system.

References

[1] P.G. Stoks, A.W. Schwartz, Cosmochim. Acta 45 (1981) 563.
[2] S.B. Charnley, Y.-J. Kuan, H.-C. Huang, O. Botta, H.M. Butner, N. Coz, D. Despois, P. Ehrenfreund, Z. Kisiel, Y.-Y. Lee, A.J. Markwick, Z. Peeters, S.D. Rodgers, Adv. Space Res. 36 (2005) 137.
[3] A. Hustrulid, P. Kush, J.T. Tate, Phys. Rev. 54 (1938) 1037.
[4] C. Fridh, L. Åsbrink, B.Ö. Jonsson, E. Lindholm, Int. J. Mass Spectrom. Ion Phys. 8 (1972) 85.
[5] M.-F. Lin, Y.A. Dyakov, C.-M. Tseng, A.M. Mebel, S.H. Lin, Y.T. Lee, C.-K. Ni, J. Chem. Phys. 123 (2005) 054309.
[6] M.-F. Lin, Y.A. Dyakov, C.-M. Tseng, A.M. Mebel, S.H. Lin, Y.T. Lee, C.-K. Ni, J. Chem. Phys. 124 (2006) 084303.
[7] E.T. Sevy, M.A. Muysken, S. Rubin, G.W. Flynn, J. Chem. Phys. 112 (2000) 5829.
[8] S.R. Goates, J.O. Chu, G.W. Flynn, J. Chem. Phys. 81 (1984) 4521.
[9] G.S. Ondrey, R. Bersohn, J. Chem. Phys. 81 (1984) 4517.
[10] T. Gejo, J.A. Harrison, J.R. Huber, J. Chem. Phys. 100 (1996) 13941.
[11] M. Schwell, H.W. Jochims, H. Baumgärtel, F. Dulieu, S. Leach, Planet. Space Sci. 54 (2006) 1073.
[12] H.-W. Jochims, M. Schwell, H. Baumgärtel, S. Leach, Chem. Phys. 314 (2005) 263.
[13] O. Plekan, V. Feyer, R. Richter, M. Coreno, M. de Simone, K.C. Prince, Chem. Phys. 334 (2007) 53.
[14] G. Vall-llosera, M. A. Huels, M. Coreno, A. Kivimäki, K. Jakubowska, M. Stankiewicz, E. Rachlew, ChemPhysChem 9 (2008) 1020.
[15] S.L. Sorensen, B.J. Olsson, O. Widlund, S. Huldt, S.-E. Johansson, E. Rachlew, A.E. Nilsson, R. Hutton, U. Litzén, A. Svensson, Nucl. Instrum. Methods Phys. Res. A297 (1990) 296.
[16] G. Vall-llosera, Synchrotron radiation studies of gas phase molecules; from hydrogen to DNA sugars, Ph.D. thesis, ISBN: 978-91-7178-852-8, 2008.
[17] Kimura, Handbook of HeI Photoelectron Spectra of Fundamental Organic Molecules, Ionization Energies, ab initio Assignments, and Valence Electron Structure for 200 Molecules, Halsted Press/Japan Societies Press, New York/Tokyo, 1981.
[18] H. Budzikiewicz, C. Djerassi, D. Williams, Mass Spectrometry of Organic Compounds, Holden-Day, San Francisco, 1967.
[19] C.Q. Jiao, C.A. DeJoseph, R. Lee, A. Garscadden, Int. J. Mass Spectrom. 257 (2006) 34.
[20] B.Ö. Jonsson, E. Lindholm, A. Skerbele, Int. J. Mass Spectrom. Ion Phys. 3 (1969) 385.
[21] M.J.S. Dewar, S.D. Worley, J. Chem. Phys. 51 (1969) 263.
[22] L. Åsbrink, C. Fridh, B.Ö. Jonsson, E. Lindholm, Int. J. Mass Spectrom. Ion Phys. 8 (1972) 215.
[23] L. Åsbrink, C. Fridh, B.Ö. Jonsson, E. Lindholm, Int. J. Mass Spectrom. Ion Phys. 8 (1972) 229.
[24] W. Reusch, Virtual textbook of organic chemistry, www.cem.msu.edu/~reusch/VirtualText/react2.htm, 1999.
[25] Y.R. Luo, Handbook of Bond Dissociation Energies in Organic Compounds, CRC Press, USA, 2003.
[26] C. Fridh, L. Åsbrink, B.Ö. Jonsson, E. Lindholm, Int. J. Mass Spectrom. Ion Phys. 8 (1972) 101.
[27] A. Peeters, O. Botta, S.B. Charnley, Z. Kisiel, Y.J. Kuan, P. Ehrenfreund, Astronom. Astrophys. 443 (2005) 583.
[28] H.W. Jochims, E. Rühl, H. Baumgärtel, S. Tobita, S. Leach, Int. J. Mass Spectrom. Ion Proc. 167/168 (1997) 35.
[29] M.N. Piancastelli, P.R. Keller, J.W. Taylor, F.A. Grimm, T.A. Carlson, J. Am. Chem. Soc. 105 (1983) 4235.
[30] A.W. Potts, D.M.P. Holland, A.B. Trofimov, J. Schirmer, L. Karlsson, K. Siegbahn, J. Phys. B: At. Mol. Opt. Phys. 36 (2003) 3129.
[31] P. Tzallas, C. Kosmidis, K.W.D. Ledingham, R.P. Singhal, T. McCanny, P. Graham, S.M. Hankin, P.F. Taday, A.J. Langley, J. Phys. Chem. A 105 (2001) 529.
[32] J.G. Philis, J. Mol. Spectrosc. 232 (2005) 26.
[33] S. E. Stein, NIST Mass Spec Data Center "Mass Spectra" in NIST Chemistry WebBook, NIST Standard Reference Database Number 69, National Institute of Standards and Technology, Gaithersburg MD, 20899 (http://webbook.nist.gov), 2005.
[34] M.N. Simon, M. Simon, Astrophys. J. 184 (1973) 757.
[35] Y.J. Kuan, C.H. Yan, S.B. Charnley, Z. Kisiel, P. Ehrenfreund, M.N.R.A.S 345 (2003) 650.
[36] O. Botta, J.L. Bada, Surv. Geophys. 23 (2002) 411.
[37] A. Peeters, O. Botta, S.B. Charnley, R. Ruiterkamp, P. Ehrenfreund, Astrophys. J. 593 (2003) 129.